Infrared Multi-Color Photometry and Polarimetry

AUTHOR(S):

Okuda, Haruyuki; Maihara, Toshinori; Sato, Shuji

Memoirs of the Faculty of Science, Kyoto University, Series of Physics, Astrophysics, Geophysics and Chemistry, Vol. XXXIV, No. 3, Article 1, 1974.

INFRARED MULTI-COLOR PHOTOMETRY AND POLARIMETRY

BY

Haruyuki OKUDA, Toshinori MAIHARA and Shuji SATO

Department of Physics, Faculty of Science, Kyoto University, Kyoto

(*Received December 16, 1972*)

ABSTRACT

A multi-color photometer has been built for ground based infrared astronomical observations in near infrared i.e. between 1 and 4 microns. A liquid nitrogen cooled lead sulphide photoconductor is used for the detector.

It can be used also for a polarimeter by inserting a rotating polarizer. The signal from the detector is recorded on a magnetic tape simultaneously with the mark indicating the rotation angle. The data are digitized by an A-D converter and analysed by computor processing.

§1. Introduction

Infrared radiation lying between visible light and radio wave; i.e. 0.7~1000 microns, could have been used for astronomical observations by development of the semi-conductor detectors with extremely high sensitivities. Since the 2-micron survey carried in 1965 by Neugebauer et al., using their 150 cm plastic mirror, various infrared sources have been discovered. The survey led to the discovery of extremely cool stars, so called infrared stars. A much cooler object, an 'infrared nebula' has been found by far infrared observations which was made possible by Low's development of the high sensitivity bolometer. Using the same detector, he has succeeded to detect quite a strong far infrared radiation in quasi stellar object and Seyfert galaxies. He has shown by further detailed observations that the energy emitted in the far infrared is many orders of magnitude larger than that emitted in any other wavelength region. Infrared observation has also unveiled the strong extinction of the interstellar dust clouds and took a close-up of the Galactic center (Becklin et al. 1968). By observations in far infrared (Becklin et al. 1969, Hoffmann et al. 1969, Aumann and Low 1970), it has revealed the existence of the intense radiation having similar spectrum with a peak near 70 μ as Q.S.O. or Seyfert galaxies. Strong infrared radiation has been also observed in novae (Hyland et al. 1970, Geisel et al., 1970).

These radiations are considered to be emitted by dense solid grains or dust particles heated by some other energy sources, but details are still unknown.

Most of these observations have been carried by ground based telescopes. Because of strong atmospheric absorption mostly due to H_2O, CO_2 and O_3 molecules, they could be done only through several wavelength bands. The transmission of infrared radiation for the standard atmosphere is shown in Fig. 1.

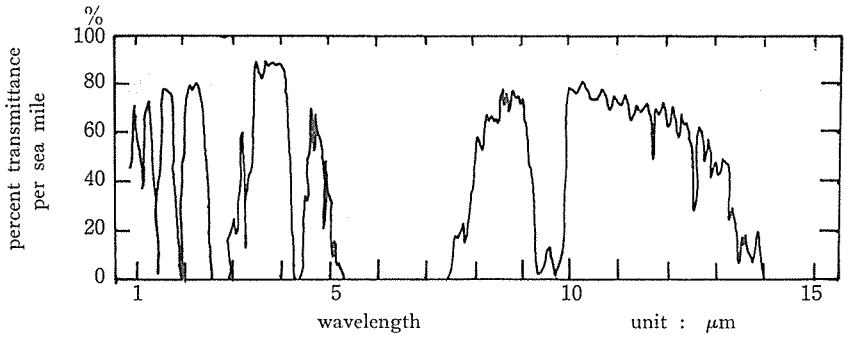

Fig. 1. Atmospheric transmission

Wavelength bands where the atmosphere is relatively transparent are called 'atmospheric windows' and distribute only in the wavelengths shorter than 20 μ. The atmosphere is, on the other hand, a strong infrared emitter in longer wavelengths which becomes serious disturbance for the observation in 5, 10, and 20 μ bands. The absorption and emission are mainly determined by the content of water vapor in the atmosphere, which is strongly dependent on the altitude and temperature. High altitude and cold climate are therefore favorable conditions for the infrared observations.

In order to observe energy spectrum of celestial infrared radiation in wide range of wavelengths and polarization in near infrared, a multicolor infrared photometer and polarimeter has been built.

§2. Photometer and Polarimeter

a. Photometer

Since the sensitivities of infrared detectors are generally not sufficiently high, poor signal to noise ratio of the direct signal from the detector must be improved by the method of synchronous rectification, which requires chopping of the radiation beam. General structure of the photometer which we have built is such as shown in Fig. 2. The radiation

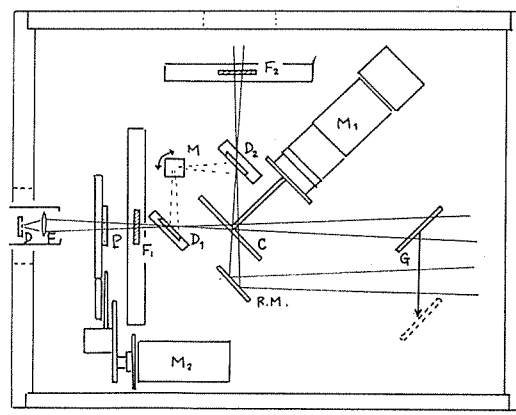

Fig. 2. Photometer

C: chopper G: mirror for guiding RM: reference mirror M_1, M_2: motors
D_1, D_2: diaphragm F_1, F_2: filters mounted on the disk P: polarizer
F: Fabry lens D: detector M: microscope for diaphragm inspection

beam collected by a telescope with focal ratio of f/13 or f/15, is chopped by a motor drived rotating blades. The rotating blades are declined by 45° to the incident beam and two types of chopping beam are available; one is a straight beam which is directly chopped by rotating blades, another is chopped after reflected perpendicularly by a fixed mirror parallel to the rotating blades. The front surface of the rotating blades is covered with mirrors so as to reflect nearby sky background radiation. The former beam is mainly used for near infrared observations which are relatively free from atmospheric emission and for polarization measurement which will be described later.

In the latter type of beam transport, the field contained the observing object and that of the neighboring sky are sent to the detector alternatively, and therefore contribution from the sky background can be cancelled by an A.C. amplification.

Chopping frequency is selected between 30 Hz and 200 Hz to give the maximum S/N ratio for each detectors. Between the chopper and the filter, is put a diaphragm with diameters of 0.5, 1, 2, 3 and 5 mm. The stainless steel diaphragms polished and aluminized are declined so as to reflect the off field which can be monitored by a microscope. Filters are mounted on a disc, rotation of which select the observing wavelength.

In front of the detector, a field lens with a diameter and a focal length of 10 mm is put to make an image of objective mirror on the sensitive area of the detector. The field lens is made of fused quartz, mounted inside the cryostat and cooled at liquid nitrogen temperature.

b. Filter system

The filters have been chosen to correspond with the atmospheric windows. Bandwidths of the filters are however, slightly narrower than those of Johnson's system (Johnson et al. 1966) to reduce the effect of atmospheric absorption which may be more serious on humid Japanese climate. The J-band in Johnson's system is also divided into two bands by the same reason. The wavelength bands thus defined are named as K-0, K-1, K-2....., from the shorter to longer wavelength. The longer wavelength edge of K-0 and K-5 bands are determined by the sensitivities of Si-photovoltaic detector and PbS-photoconductive detector respectively. The characteristics of the filter system are summarized and compared with the Johnson's one in Table 1 and the filter transmission curves are shown in Fig. 3 superposing on the atmospheric transmission. Transmission curves of the Johnson's filter system are also shown in Fig. 4, for comparison.

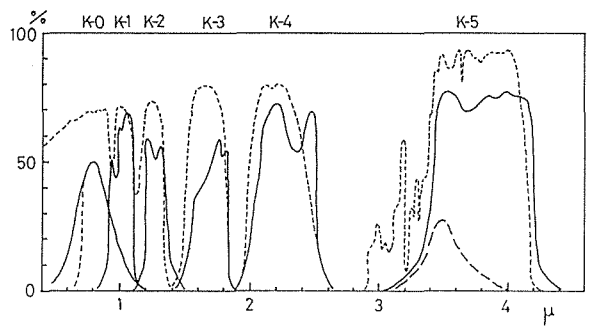

Fig. 3. Filter system

—— transmission of filter, ------ atmospheric window —— Filter transmission multiplied by the detector sensitivity.

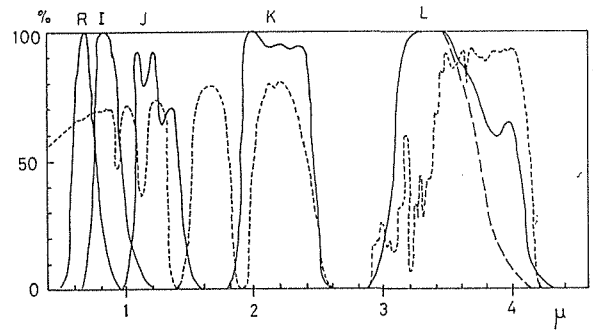

Fig. 4. Filter system of Johnson's peak transmissions of filters are normalized to 100.

—— filter transmission, ····· atmospheric transmission,
—— filter transmission multiplied by the detector sensitivity.

Table 1. Filter System

Band	K-0	K-1	K-2	K-3	K-4	K-5	K-6	K-7
$\lambda\lambda$ (μ)	0.7–0.9*	0.9–1.1	1.2–1.4	1.5–1.8	2.0–2.5	3.3–3.7*	4.6–5.1	8.5–14
$\Delta\lambda$ (μ)	0.2	0.2	0.2	0.3	0.5	0.4	0.5	5.5
λ_0 (μ)	0.8	1.0	1.3	1.65	2.25	3.5	4.8	11
Johnson	I		J	H	K	L	M	N

* Filter transmission x detector sensitivity

Table 2. Conversion factors of absolute flux

Band	K-0	K-1	K-2	K-3	K-4	K-5	K-6	K-7	
Absolute flux for mag.=0.0	1.13×10^{-12}	6.1×10^{-13}	2.9×10^{-13}	1.2×10^{-13}	3.8×10^{-14}	7.2×10^{-15}	2.5×10^{-15}	9.5×10^{-17}	W/cm$^2\mu$

c. Detectors

A Si-photovoltaic detector with 5 mm diameter is used for observation in K-0 band. Its sensitivity has a maximum near 0.85 μ (NEP$\sim10^{-13}$ W) and decreases rapidly with wavelength. The sensitivity in shorter part is blocked by a glass filter VR-69 which is fixed on the surface of the detector. For observations from K-1 to K-5 bands, a liquid nitrogen cooled PbS photoconductive detector is used. The sensitive area is 1×1 mm^2

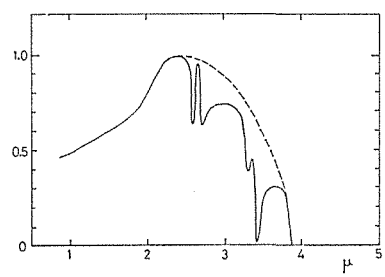

Fig. 5. Overall sensitivity of the PbS detector cooled by liquid nitrogen with Fabry lens of fused quartz.

and its NEP is about 10^{-13} W at maximum sensitivity. The wavelength dependence of the sensitivity is illustrated in Fig. 5. The cryostat for cooling the detector is shown in Fig. 7. The temperature of the detector is kept constant independently with the attitude of the cryostat as long as 10 hours by a single filling of 500 cc liquid nitrogen.

A mercury-doped Ge photoconductive detector cooled by liquid He was tried to use for K-6 and K-7 bands. The NEP of the detector is however a little better than 10^{-11} W. Only bright objects could be observed. It will be replaced by a Ge-In bolometer which will cover observations in K-5, K-6 and K-7 bands.

d. Polarimeter

The photometer can be used as a polarimeter in which a polarizer, HR-type polaroid, is inserted between the filter and the detector. The straight beam is used in this case in order to avoid the spurious polarization by reflection on the chopping mirror. The polarizer is mounted on a rotating ring which is drived by a motor with a constant speed, varying from 0.2 rpm to 2 rpm. Observations of many times iterations improve the accuracy of the measurement a great deal so that faint objects or small degree of polarization can be measured. Rotation angle of the polarizer is measured by a mark signal from an electrical contact of a point on the ring. The characteristics of polarizer are shown in Fig. 6.

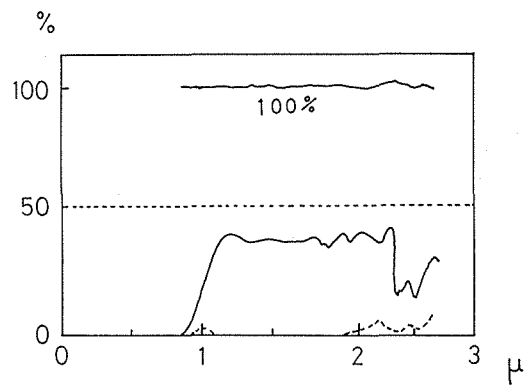

Fig. 6. Characteristics of HR polarizer.
—— transmission of a single plate.
····· transmission of double plates crossed perpendicularly.

§3. Electronic Devices

Photometric and polarimetric measurements have been so far carried on by means of a high sensitive PbS detector of Infrared Company. This PbS element shows a resistivity of several hundred kiloohms at room temperature, and the dark resistivity becomes as much as some ten megohms when it is cooled at liquid nitrogen temperature. Therefore electronic devices should consist of a high input impedance pre-amplifier having a very low noise level. Besides the system should contain a synchronous rectifier referred to the chopping sign in an adequate modulation frequency.

The early electronic circuit system designed and constructed for the purpose of infrared photometry has been reported in ref. 7, but in our recent observations we can mainly use a lock-in-amplifier Type "HR-8" of P.A.R. Company. Fig. 8 shows a block

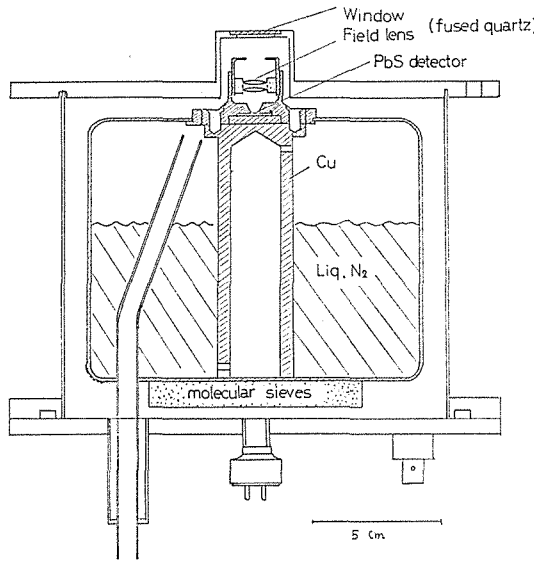

Fig. 7. Inner structure of the liquid nitrogen cryostat.

diagram of the electronic devices in the usual multicolor photometry.

As shown in Fig. 8, a confronted diode pair; a gariumarsenide emission diode and a silicon photo-sensitive diode (a solar battery), generates the reference signal of the chopping frequency. These semiconductor elements however, cause to drift the reference signal level as the environmental temperature varies, and moreover thus emitted radiation whose spectrum has a sharp maximum near 9000 Å may give error responses on the detector by the stray light. The latter effect may be a severe problem especially in the polarization

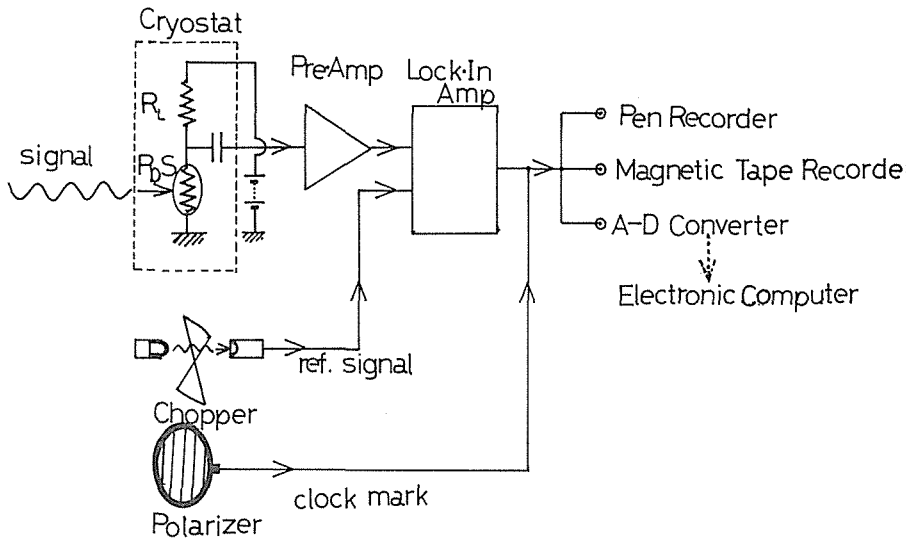

Fig. 8. Block diagram of the electronic devices

measurement at K-1 band. We must have reduced the current of the GaAs diode to eliminate such an interference.

To measure the linear polarization of infrared objects we observe a periodic signal from the detector as the polarizer rotates continuously. But usually we cannot recognize the value of polarization from the data of only one rotation owing to the insufficient signal to noise ratio (For example the ratio of the infrared intensity at K-4 band of the Galactic center is less than ten after the polarizer being inserted, even when the detector is attached to the 74" reflector in the Okayama Astrophysical Observatory.) So we have tried to superpose signal of many succeeding rotations of the polarizer to improve the signal to noise ratio.

In the early practical method of superposition we used a four-channel analogue data recorder in the following way. A data of one period of rotation (about two or three minutes) is recorded on one of four tracks in FM modulation, then after rewinded back to the initial part, a new data of next rotation is added to the preceding data played back from the recorder. The summed up signal is recorded to the neighboring track. This method however, cannot avoid considerable loss time for rewinding the tape and switching input and output channels of the recorder.

At present we record the successive periodic signal continuously on the analogue data recorder along with a clock pulse signal generated in every rotation. Superposition of the data is carried out after digitization by an A-D converter, and analysed numerically by a computer. This method can avoid loss time of observation of the former method.

§4. Data processing

1. Photometry

a. Basic procedure

Principally the absolute intensity of the observed object can be estimated by comparing the observed signals with those of comparison stars, the absolute intensities of which had been previously determined.

Let S_{obj} be the signal of the object in a certain band, S_{comp} be that of a comparison star, the absolute intensity of the observing object I_{obj} is calculated by

$$I_{obj}=I_{comp}\times(S_{obj}/S_{comp}), \tag{1}$$

where I_{comp} is the absolute intensity of the comparison star. Rigorously, however, this is allowed only when they are observed by the same system carried in determination of the intensities of the comparison stars, i.e. by the same filter transmission, the same detector sensitivity and by the same atmospheric conditions. For comparison stars, we have selected from Johnson's observations of bright stars. (Johnson et al. 1966) As described in §2, our filter system is slightly different from that of Johnson's.

Taking these difference into account, we adopt the following value for I_{comp},

$$I_{comp}=\int_0^\infty I(\lambda)F(\lambda)S(\lambda)d\lambda/\int_0^\infty F(\lambda)S(\lambda)d\lambda, \tag{2}$$

where $F(\lambda)$ is the transmission of the filter and $S(\lambda)$ represents the sensitivity of the detector of our system. $I(\lambda)$ means the energy spectrum of the comparison star. This is, however, given only discretely at special wavelengths or bands namely U, B, V, R, I, J, K and L. Approximating $I(\lambda)$ by a parabolic function which connects the given intensity with those of

neighbor points of both sides, we calculate I_{comp} by eq. (2), substitution of which into eq. (1) gives the absolute intensity of the object I_{obj}. Comparison stars are chosen to be nearest neighbors to the observing object and measured before and after the observation of the object, so as to make the observing conditions as similar as possible.

b. Selection of comparison stars

Johnson has carried multi-color photometry of more than 1500 bright stars, magnitudes of which are given at U, B, V, R, I, J, K and L in his catalogue (Johnson et al. 1966). About 50 stars which had been frequently measured are selected from his catalogue for comparison stars. They are brighter than 0 magnitude at K-band and belong mostly to K and M type stars but limited only to non-variable stars. Their effective absolute intensity calculated by eq. (2) are listed in Table 2. Conversion factors between absolute intensities and magnitude given in Table 2, are used in the calculation.

The intensities at H-band (K-3 in our system) have not been given in Johnson's catalogue. We estimated by interpolating J and K-band intensities. But they must be corrected for H^--excess which will be discussed later.

c. Atmospheric correction

Infrared radiation is extinguished by atmospheric absorption mainly due to water vapor. As the comparison stars are chosen to be as close as possible to the observing object, the effects of the atmospheric extinction for both observations are almost the same and approximately taken out automatically by adopting the eq. (1). It is, however, necessary for rigorous discussions to correct the effect more seriously. When the extinction is not extremely large, the reduction factor of the intensity can be approximately given by

$$I_\lambda(z)=I_\lambda{}^0 e^{-\tau_\lambda}, \tag{3}$$

where $I_\lambda(z)$ is the intensity at a wavelength λ observed at a zenith angle of z. $I_\lambda{}^0$ indicates the intensity before entrance into the atmosphere. τ_λ is the optical depth for radiation at λ and approximately proportional to sec z so long as it is small i.e.

$$\tau_\lambda=k_\lambda \sec z, \tag{4}$$

where k_λ is a constant dependent on the wavelength as well as the atmospheric conditions.

The reduction magnitude can be given from eq. (3) and (4)

$$\begin{aligned} &\ln(I_\lambda(z)/I_\lambda{}^0)=-k_\lambda \sec z \quad \text{or} \\ &\Delta m=-1.09 k_\lambda \sec z. \end{aligned} \tag{5}$$

The value of k_λ can be obtained empirically from the gradient of Δm vis sec z curve, which is plotted by observations of a number of comparison stars of known intensities at various zenith angles. Example of the extinction curves are shown in Fig. 9. As seen in the figures, the curves are almost straight, which ascertain the assumption adopted above. If the value of k_λ is known from these curves, the absolute intensity of the observing object can be easily estimated by eq. (1), replacing S_{obj} and S_{comp} by $S_{obj} \exp(-k_\lambda \sec z_{obj})$ and $S_{comp} \exp(-k_\lambda \sec z_{comp})$.

Large dispersion of points in Fig. 9(c), is significant and can be explained by the reason discussed below.

d. Correction due to H^--excess

As has been mentioned above, the large dispersion is noticeable in the plots of Fig.

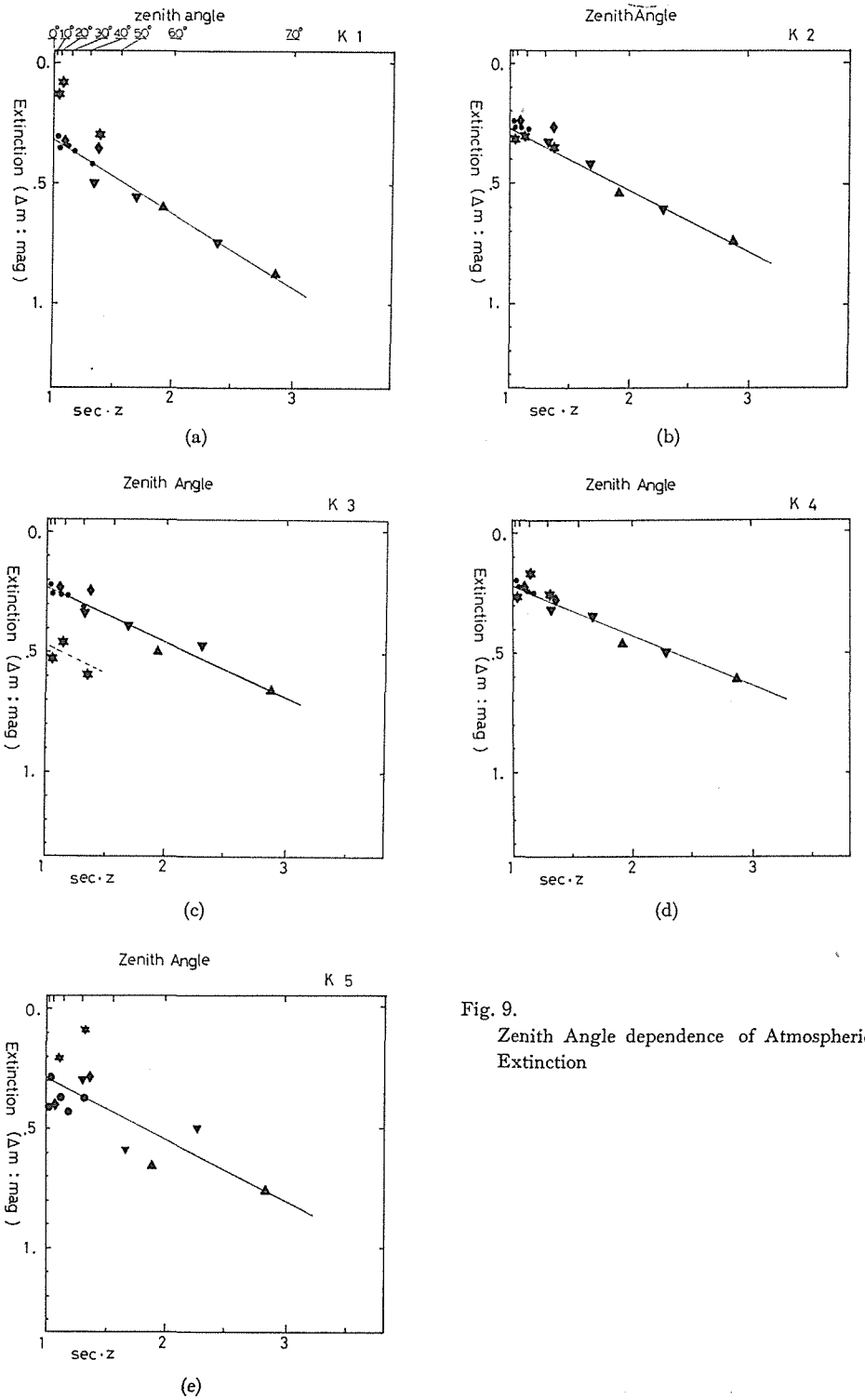

Fig. 9.
Zenith Angle dependence of Atmospheric Extinction

9(c). Careful inspection shows that the intensities depend on the spectral type of the comparison stars, i.e. intensity increases as the type of star advances. We have estimated the intensities at H-band by interpolation of J and K-bands intensities, for no data is given in Johnson's. This assumption is valid only for early type stars, spectra of which are free from modulation due to molecular absorptions typical in near infrared region. The excess of intensities from the interpolated values are plotted in Fig. 10, by assuming that there is no excess in A-type stars.

The results shown in Fig. 10 means that the intensities of late type stars are enhanced

Table 3. Flux of Standard Stars unit: W/cm^2·μ

			K0	K1	K2	K3	K4	K5
α	Cas	K0	4.07(−13)	3.06(−13)	2.31(−13)	1.50(−13)	4.59(−14)	1.07(−14)
β	Cet	K0	4.50(−13)	3.16(−13)	2.37(−13)	1.53(−13)	4.91(−14)	7.11(−15)
β	And	M0	9.84(−13)	9.13(−13)	7.24(−13)	4.23(−13)	1.97(−13)	3.94(−14)
γ	And	K0	5.63(−13)	4.41(−13)	3.34(−13)	2.51(−13)	7.68(−14)	1.63(−14)
α	Ari	K2	5.39(−13)	4.10(−13)	3.10(−13)	1.68(−13)	6.56(−14)	1.44(−14)
α	Cet	M0	7.98(−13)	7.71(−13)	5.91(−13)	4.73(−13)	1.72(−13)	3.57(−14)
ϵ	Eri	K2	9.14(−14)	6.16(−14)	4.32(−14)	2.66(−14)	7.60(−15)	1.76(−15)
γ	Eri	K5	4.42(−13)	4.07(−13)	3.19(−13)	2.34(−13)	8.60(−14)	1.81(−14)
α	Tau	K5	2.79(−12)	2.45(−12)	1.85(−12)	1.32(−12)	4.87(−13)	1.15(−13)
ϵ	Lep	K5	2.61(−13)	2.27(−13)	1.83(−13)	1.31(−13)	4.48(−14)	7.78(−15)
β	Ori	B8	1.04(−12)	4.61(−13)	2.78(−13)	1.07(−13)	3.24(−14)	5.97(−15)
α	Aur	G8	2.34(−12)	1.58(−12)	1.12(−12)	5.76(−13)	1.87(−13)	3.88(−15)
β	Lep	G0	1.90(−13)	1.28(−13)	9.28(−14)	4.88(−14)	1.72(−14)	2.24(−15)
μ	Gem	M0	8.50(−13)	9.06(−13)	7.10(−13)	4.37(−13)	2.08(−13)	4.15(−14)
γ	Gem	A0	2.11(−13)	9.53(−14)	5.91(−14)	2.29(−14)	6.78(−15)	6.60(−16)
α	CMa	A0	4.45(−12)	1.95(−12)	1.17(−12)	4.42(−13)	1.30(−13)	2.28(−14)
α	Gem	A1	2.88(−13)	1.31(−13)	8.16(−14)	3.19(−14)	9.53(−15)	1.74(−15)
α	CMi	F5	1.32(−12)	7.52(−13)	4.91(−13)	2.12(−13)	7.03(−14)	1.29(−14)
β	Gem	K0	1.04(−12)	7.17(−13)	5.34(−13)	3.37(−13)	9.90(−14)	2.14(−14)
α	Lyn	K5	3.07(−13)	2.76(−13)	2.37(−13)	1.73(−13)	6.41(−14)	1.43(−14)
α	Hya	K2	7.43(−13)	6.07(−13)	4.61(−13)	3.28(−13)	1.09(−13)	2.45(−14)
α	Leo	B7	3.15(−13)	1.34(−13)	8.16(−14)	3.06(−14)	8.77(−15)	1.60(−15)
γ	Leo	K0	5.55(−13)	4.19(−13)	3.13(−13)	2.11(−13)	6.81(−14)	1.49(−14)
γ	Vir	F0	1.28(−13)	7.31(−14)	4.96(−14)	2.15(−14)	6.39(−15)	1.32(−15)
δ	Vir	M3	4.93(−13)	5.12(−13)	3.98(−13)	3.12(−13)	1.16(−13)	2.71(−14)
ϵ	Vir	K0	1.89(−13)	1.29(−13)	9.72(−14)	6.07(−14)	1.73(−14)	3.64(−15)
α	Vir	B2	3.89(−13)	1.47(−13)	8.79(−14)	3.01(−14)	8.30(−15)	1.51(−15)
α	Boo	K2	4.27(−12)	3.18(−12)	2.53(−12)	2.02(−12)	5.78(−13)	1.31(−13)
ϵ	Boo	K0	3.37(−13)	2.42(−13)	1.87(−13)	1.23(−13)	3.60(−14)	7.60(−15)
σ	Lib	M3	5.27(−13)	5.46(−13)	4.28(−13)	3.51(−13)	1.33(−13)	3.14(−14)
α	Ser	K0	2.77(−13)	2.12(−13)	1.69(−13)	1.13(−13)	3.44(−14)	7.17(−15)
α	Lyr	A0	1.07(−12)	5.01(−13)	3.34(−13)	1.33(−13)	3.83(−13)	7.13(−15)
δ	Lyr	M4	3.52(−13)	4.12(−13)	3.44(−13)	2.92(−13)	1.14(−13)	2.76(−14)
β	Cyg	K0	2.10(−13)	1.68(−13)	1.34(−13)	9.49(−14)	3.15(−14)	6.99(−15)
γ	Sgr	K0	1.86(−13)	1.32(−13)	1.02(−13)	6.63(−14)	2.14(−14)	3.02(−15)
λ	Sgr	K2	2.25(−13)	1.69(−13)	1.30(−13)	8.55(−14)	2.75(−14)	3.76(−15)
α	Cyg	A2	4.34(−13)	2.13(−13)	1.35(−13)	5.51(−14)	1.59(−14)	3.43(−15)
ϵ	Cyg	K0	3.09(−13)	2.21(−13)	1.67(−13)	1.85(−13)	3.28(−14)	7.14(−15)
ξ	Cyg	K5	1.92(−13)	1.71(−13)	1.35(−13)	9.96(−14)	3.84(−14)	8.97(−15)
ϵ	Peg	K2	5.04(−13)	4.20(−13)	3.31(−13)	2.21(−13)	7.63(−14)	1.32(−14)
λ	Agr	M2	2.72(−13)	2.78(−13)	2.27(−13)	1.90(−13)	6.96(−14)	1.41(−14)
α	PsA	A3	4.29(−13)	2.04(−13)	1.33(−13)	5.34(−14)	1.60(−14)	1.47(−15)

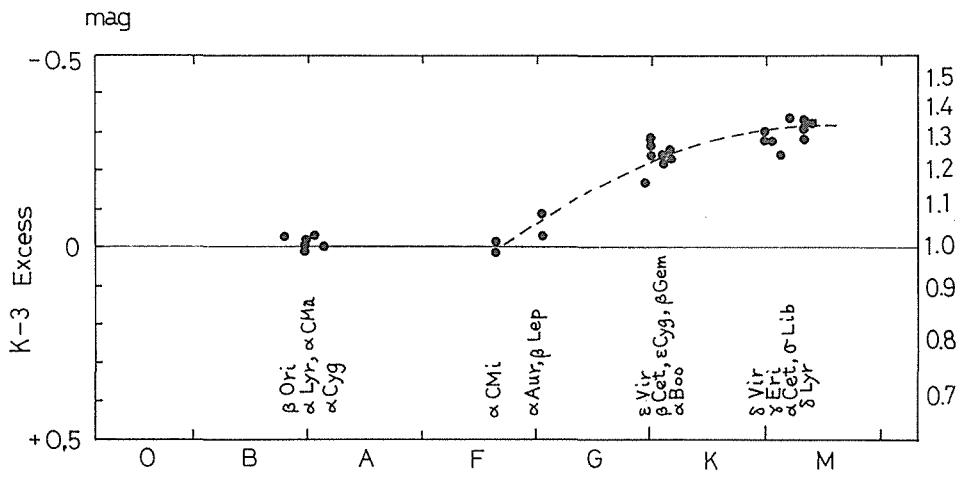

Fig. 10. Spectral dependence of H^- excess

Table 4. Correction factor for H^--excess

Sectral type	B	A	F	GO	G5	KO	K5	MO	M5
mag	0.00	0.00	0.00	0.07	0.14	0.22	0.28	0.31	0.32
multiplication factor	1.00	1.00	1.00	1.07	1.14	1.22	1.29	1.32	1.33

somewhat at K-3 band or making humps in the spectra near 1.6 microns. Such a hump can be explained by decrement of absorption coefficient near 1.6 microns of H^--ions which can be present in the atmosphere of the late type stars with temperature less than 4000°K (Tsuji, 1966). The absolute intensities of comparison stars at H-band or K-3 band are reestimated using the above results and added in Table 3.

e. Tape recording and computor processing

When the signal from the object is so weak as the level of detector noise, longer integration time is necessary to get good signal to noise ratio. In that case, we record the output signals from the observing object and from the neighboring sky on magnetic tape alternatively with an interval of a minute or so. The signals recorded for a number of iterated observations are digitized by an A-D converter and punched on a paper tape which is later analysed by an electronic computor (KDC-II in Kyoto Univ.). This proceesing can easily improve the minimum detectable power by an order of magnitude.

2. Polarimetry

Since thep olarization is generally very small and invisible in a single rotation measurement, the observation is iterated for a number of rotations to improve statistics. The recorded signal are digitized with a constant sampling rate, about once a second and punched on the paper tape. The data thus prepared for a series of iterations are processed by an electronic computor KDC-II in Kyoto University. They are added up by adjusting their phase referring to the clock pulse. The Fourier components of the first, second, and fourth orders are derived from the superposed data by method of least square, i.e.

$$I(\theta)=I_0+I_1\sin(\theta+\delta_1)+I_2\sin(2\theta+\delta_2)+I_4\sin(4\theta+\delta_4). \quad (4)$$

Degree of polarization is given by

$$P=I_2/I_0\times 100\%,$$

and the position angle of the polarization is obtained by

$$P.A=\delta_0+\delta_2/2.$$

where δ_0 is the position angle for the starting clock mark. For pure polarization, the second and fourth terms in eq. (4) should be absent. We can check spurious polarization of instrumental or statistical origins from the order of magnitudes of their terms.

Spurious or instrumental polarization can be also monitored by measuring bright stars which are known to be unpolarized. Several stars such as α Boo, α Tau, α Lyr and αOri have been measured for this purpose. The measured polarizations range around 0.5%.

§5. Discussions

Since 1968, several observations were carried out by attaching the photometer and the polarimeter to the 36" and 74" reflectors in Okayama Astrophysical Observatory. Infrared brightness and polarization of the Moon were measured in 1968. From the phase angle dependences of the brightness and polarization, the surface of the Moon was estimated to be consisted of small dust powder of size as large as 10 μ. This conclusion was fully proved by the Appolo's exploration performed in next year. Albedos of the planets; Venus, Mars, Jupiter and Saturn were also measured and shown to be of great variety in different type of planets. Energy spectra of late type stars and infrared stars which had been discovered a little before and their time variations were measured especially for long period variable stars. A series of observations has shown that energy spectra of late type stars are considerably anomalous, deviating from the Planckian spectrum especially in the case of carbon stars, and that the changes in infrared intensity of the long period variables are relatively small, mostly less than a factor of 2, while those in the visible range amount as large as two orders of magnitudes. It was also found that infrared stars vary in their intensitites.

In 1970, the polarization measurement was tried for an infrared star VY CMa, and resulted in the discovery of large and anomalous infrared polarization (Hashimoto et al., 1970). This peculiar polarization is explained by scattering by a dense circumstellar dust cloud which is distributed elongated around the central star. The similar polarization was also observed in another infrared star IRC+10216 by later measurements, (Maihara et al., 1971).

Infrared polarization has been searched in the Galactic center source at 2 μ band in 1969, 1970 and 1971. From the observations in later two years, finite values of polarization of several percent were measured (Maihara et al., 1971), although poor signal to noise ratio of the measurement due to extremely weak intensity of the source cannot make it conclusive yet.

In the course of these observations, the following problems have been found to be improved:

A relatively large fluctuation is seen in the output signal due to wandering of the star image in the diaphragm. This might be caused by some imperfect adjustment in the

axis of the detector system; i.e. the detector and the field lens axis, in the cryostat.

The background atmospheric radiation appears from the observations beyond K-5 band. Such background radiation can be reduced about an order of magnitude in K-5 (3.5 μ) band by the method of reflecting mirror chopper. Much more careful and complete cancellation must be applied, for example, by vibrating the secondary mirror in Cassegrain telescope.

Spurious polarization by instrumental origin amounts to several tenth percent which depends on how to adjust the detector axis. Since the position angle of the spurious polarization changes as the detector rotates, it may be in some part due to anisotropic sensitivity of the detector to the polarized radiation.

The HR type polaroid works as a perfect polarizer only between 0.8 μ and 2.2 μ, but imperfectly in larger wavelengths up to 3 μ. From the laboratory calibration, a factor of 1.3$\sim$1.4 must be multiplied to the measured degrees of polarization in K-4 band, to get genuine polarization of the source.

In order to determine detailed characteristics of the dust clouds which originate the infrared polarization, the wavelength dependence of the polarization is desired to be observed in wide range of wavelengths. A wire mesh polarizer has been tried successfully by Forbes, for the observations beyond 2 μ, i.e. 2.2 μ band and 3.5 μ band.

Observations in far infrared region are of great importance to detect the thermal radiation of the dust cloud and its composition. Highly sensitive bolometers are now under development using Ge-In and Si elements.

REFERENCES

E. E. Becklin and G. Neugebauer 1968 Astrophys. J. **151** 145
E. E. Becklin and G. Neugebauer 1969 ibid, **157** L31
W. F. Hoffmann and C. L. Frederick 1969 ibid, **155** L 9
H. H. Aumann and F. J. Low 1970 ibid, **159** L159
A. R. Hyland and G. Neugebauer 1970 ibid, **160** L177
S. L. Geisel, D. E. Kleinmann and F. J. Low 1970 Astrophys. J. **161** L101
J. Hashimoto, T. Maihara, H. Okuda and S. Sato 1970 Pub. Astron. Soc. Japan **22** 335
T. Maihara, H. Okuda and S. Sato 1971 Proc. 17th Liege Symposium
H.L. Johnson, R.I. Mitchell, B. Iriarte and W.Z. Wisniewski 1966 Comm. Lunar and Planetary Laboratory Vol. 4 part 3, No. 63, 99.
T. Tsuji 1966, Publ. Astron. Soc. Japan **18**, 127.